Title

MiRP1 Forms IKr Potassium Channels with HERG and Is Associated with Cardiac Arrhythmia

Journal

Cell, 97(2)

ISSN

0092-8674

Authors

Abbott, Geoffrey W

Sesti, Federico

Splawski, Igor

et al.

Publication Date

1999-04-01

DOI

10.1016/s0092-8674(00)80728-x

Cell, Vol. 97, 175–187, April 16, 1999, Copyright ©1999 by Cell Press

MiRP1 Forms I_{Kr} Potassium Channels with HERG and Is Associated with Cardiac Arrhythmia

Geoffrey W. Abbott,*‖ Federico Sesti,*‖ Igor Splawski,†‖ Marianne E. Buck,* Michael H. Lehmann,‡ Katherine W. Timothy,† Mark T. Keating,† and Steve A. N. Goldstein*§

*Departments of Pediatrics and Cellular and Molecular Physiology
Boyer Center for Molecular Medicine
Yale University School of Medicine
New Haven, Connecticut 06536
†Department of Human Genetics
Howard Hughes Medical Institute
University of Utah
Salt Lake City, Utah 84112
‡Department of Internal Medicine
University of Michigan and VA Medical Center
Ann Arbor, Michigan 48109

Summary

A novel potassium channel gene has been cloned, characterized, and associated with cardiac arrhythmia. The gene encodes MinK-related peptide 1 (MiRP1), a small integral membrane subunit that assembles with HERG, a pore-forming protein, to alter its function. Unlike channels formed only with HERG, mixed complexes resemble native cardiac I_{Kr} channels in their gating, unitary conductance, regulation by potassium, and distinctive biphasic inhibition by the class III antiarrhythmic E-4031. Three missense mutations associated with long QT syndrome and ventricular fibrillation are identified in the gene for MiRP1. Mutants form channels that open slowly and close rapidly, thereby diminishing potassium currents. One variant, associated with clarithromycin-induced arrhythmia, increases channel blockade by the antibiotic. A mechanism for acquired arrhythmia is revealed: genetically based reduction in potassium currents that remains clinically silent until combined with additional stressors.

Introduction

Molecular, genetic, and physiologic studies indicate that *HERG* encodes the pore-forming subunit of cardiac I_{Kr} channels; its inheritance in mutant form is associated with long QT syndrome (LQTS), a disorder that predisposes to torsades de pointes and ventricular fibrillation (Curran et al., 1995; Sanguinetti et al., 1995). While channels formed of HERG subunits are similar in function to native I_{Kr} channels, they differ in their gating, single-channel conductance, regulation by external K^+, and sensitivity to antiarrhythmic medications (Shibasaki, 1987; Scamps and Carmeliet, 1989; Sanguinetti and Jurkiewicz, 1992; Yang et al., 1994; Sanguinetti et al., 1995; Trudeau et al., 1995; Veldkamp et al., 1995; Ho et al., 1996; Howarth et al., 1996; Spector et al., 1996a; Wang et al., 1997b; Zou et al., 1997; Ho et al., 1998; Zhou et al., 1998). This led to the hypothesis that HERG might assemble with an additional subunit to form native I_{Kr} channels (Sanguinetti et al., 1995). Here, we describe MinK-related peptide 1 (MiRP1), a subunit of 123 amino acids and a single predicted transmembrane segment. MiRP1 forms stable assemblies with HERG. The resulting channel complex has functional attributes like those of native, cardiac I_{Kr} channels. Missense mutations in the gene for MiRP1 are associated with inherited and acquired arrhythmia and changes in channel function.

Torsades de pointes (TdP) is an arrhythmia that predisposes to ventricular fibrillation (VF) and sudden death. It is associated with prolongation of the cardiac action potential due to inherited ion channel defects (Curran et al., 1995) and is a recognized risk of medications that inhibit cardiac potassium channels (Roden, 1998). Drug-induced TdP is a particularly difficult clinical problem because its occurrence is unpredictable. To assess the potential role for MiRP1 in rhythm disturbances, we screened 250 patients without mutations in the known arrhythmia genes *KVLQT1*, *HERG*, *SCN5A*, and *KCNE1* (20 with drug-induced arrhythmia and 230 with inherited or sporadic arrhythmias). Three missense mutations and a rare polymorphism were found in the gene for MiRP1. Channels formed with mutant MiRP1 subunits and HERG showed slower activation, faster deactivation, and increased drug sensitivity. These findings support a theory for arrhythmogenesis that invokes superimposition of genetic and environmental factors acting in concert to progressively diminish the capacity of cardiac ion channels to terminate each action potential in normal fashion (Roden, 1998).

Results

MinK is a short integral membrane peptide that assembles with the pore-forming subunit KvLQT1 to generate I_{Ks} channels (Takumi et al., 1988; Sanguinetti et al., 1996b). Through intimate association of its single transmembrane segment and the channel pore, MinK endows the I_{Ks} complex with slow gating kinetics, large unitary conductance, sensitivity to second messengers, and affinity for class III antiarrhythmic agents (Takumi et al., 1988; Goldstein and Miller, 1991; Blumenthal and Kaczmarek, 1994; Sanguinetti et al., 1996b; Busch et al., 1997; Sesti and Goldstein, 1998; Tai and Goldstein, 1998). While MinK can assemble with HERG, it is not the hypothetical subunit required to form native I_{Kr} channels; MinK acts only to alter the fraction of active HERG channels in the plasma membrane but does not modify their functional attributes (McDonald et al., 1997). Based on these observations, we sought to identify potential HERG-associated channel subunits by searching databases for known or predicted amino acid sequences similar to MinK.

§To whom correspondence should be addressed (e-mail: steve.goldstein@yale.edu).
‖These authors contributed equally to this work.

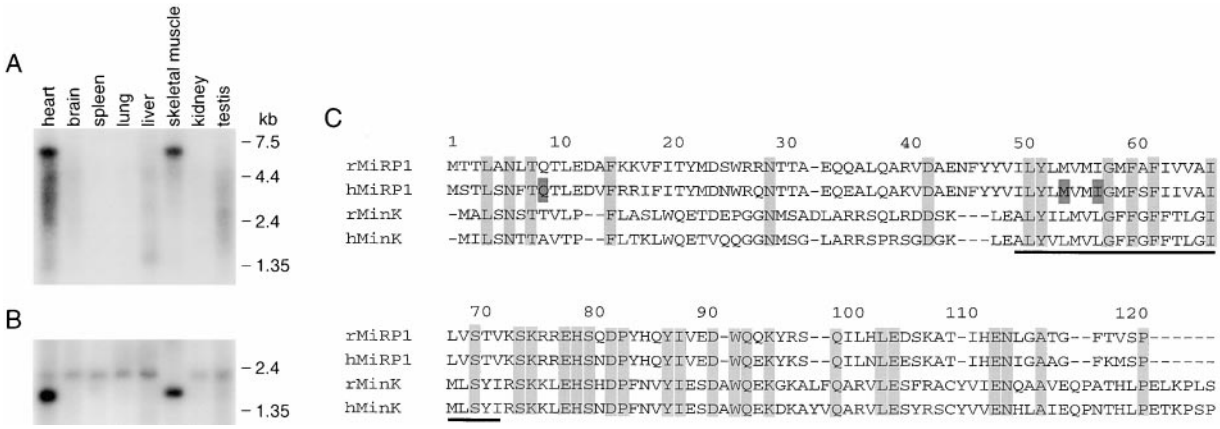

Figure 1. MiRP1 Is Expressed in the Heart and Related to MinK

(A) Rat MiRP1 tissue distribution. Northern blot of indicated rat tissues performed with an *rKCNE1* fragment (accession number D85797, 387 bp); 2 μg of poly(A)$^+$ mRNA per tissue per lane.

(B) The blot in (A) probed for β-actin.

(C) Predicted peptide sequences for rat and human MiRP1 and MinK. The putative transmembrane segment is underlined; identical residues are lightly shaded; three hMiRP1 positions associated with arrhythmia are darkly shaded (Q9, M54, and I57). MiRP1 contains consensus sequences for two N-linked glycosylation sites (N6 and N29) and two protein kinase C–mediated phosphorylation sites (T71 and S74). Rat and human *KCNE1* cDNAs contain in-frame termination codons without intervening ATGs in their 5′ upstream sequences and an A in the position −3 relative to the predicted initiator methionine; accession numbers for human and rat *KCNE1* are AF071002 and AF071003, respectively.

Identification and Cloning of Genes Encoding Products Related to MinK

Databases available through the National Center for Biotechnology Information (NCBI) were assessed for MinK-related sequences. Our search strategy targeted sites in MinK known to influence I_{Ks} channel gating (Takumi et al., 1991; Splawski et al., 1997), ion selectivity (Goldstein and Miller, 1991; Tai and Goldstein, 1998), unitary conductance (Sesti and Goldstein, 1998), pore blockade (Goldstein and Miller, 1991; Wang et al., 1996; Tai and Goldstein, 1998), and those physically exposed in the I_{Ks} channel conduction pathway (Wang et al., 1996; Tai and Goldstein, 1998). In this way, fragments of MinK-related genes were identified on nine expressed sequence tags (ESTs) and three novel genes cloned (Experimental Procedures). As the gene for MinK is designated *KCNE1*, the novel genes have been named *KCNE2*, *KCNE3*, and *KCNE4* and their nucleotide and predicted protein sequences deposited with the NCBI (Experimental Procedures). Here, we consider MiRP1, the *KCNE2* gene product.

MiRP1 Is an Ion Channel Subunit

As an EST gene fragment encoding rat MiRP1 (rMiRP1) detected an abundant single message in rat heart and skeletal muscle by Northern blot analysis (Figure 1A), a cardiac cDNA library was screened and multiple identical rMiRP1 clones were isolated (Experimental Procedures). A predicted open reading frame of 369 bp forecasts a protein of 123 amino acids with two N-linked glycosylation sites, a single transmembrane segment, and consensus sequences for two protein kinase C–mediated phosphorylation sites (Figure 1C). This suggests MiRP1 has the same simple type 1 membrane topology found for MinK—an extracellular amino terminus followed by a single membrane-spanning stretch and a cytoplasmic carboxyl terminus (Busch et al., 1992; Blumenthal and Kaczmarek, 1994; Wang and Goldstein, 1995). Rat isolates of MiRP1 and MinK show 27% amino acid identity and 45% homology (Figure 1C).

To test whether rMiRP1 could function as an ion channel subunit, its cRNA (1–25 ng) was injected into *Xenopus laevis* oocytes. Complementary RNA for MinK induces K^+ currents under these conditions by its association with a pore-forming subunit endogenous to the cells (Blumenthal and Kaczmarek, 1994; Wang and Goldstein, 1995; Sanguinetti et al., 1996b; Tai et al., 1997). In contrast, measurements by two-electrode voltage clamp revealed no currents on days 1–14 following injection with cRNA for rMiRP1 (n = 45, data not shown). Moreover, cRNA for rMiRP1 had no apparent effect on channels formed by expression of KvLQT1, KCNQ2, Shaker, fast inactivation-removed (Δ6–46) Shaker, Kv1.3, Kv1.5, Kv1.6, or Kv2.1 subunits (n = 15–39, data not shown). Conversely, rMiRP1 had significant effects on the properties of channels formed with HERG subunits.

HERG channels open when depolarized to positive voltages that favor outward K^+ currents. They are described as inwardly rectifying, however, because net ion movement through these channels is inward over a depolarization–hyperpolarization cycle when K^+ concentrations on both sides of the membrane are the same (a nonphysiologic condition routinely used for channel characterization). As seen in recordings performed in symmetrical 100 mM KCl solution (Figure 2), and modeled below, inward rectification results from rapid channel inactivation (Shibasaki, 1987; Sanguinetti et al., 1995; Trudeau et al., 1995; Smith et al., 1996; Wang et al., 1997a; Zou et al., 1997).

$$C \underset{d}{\overset{a}{\rightleftarrows}} O \underset{c}{\overset{b}{\rightleftarrows}} I \qquad \text{model}$$

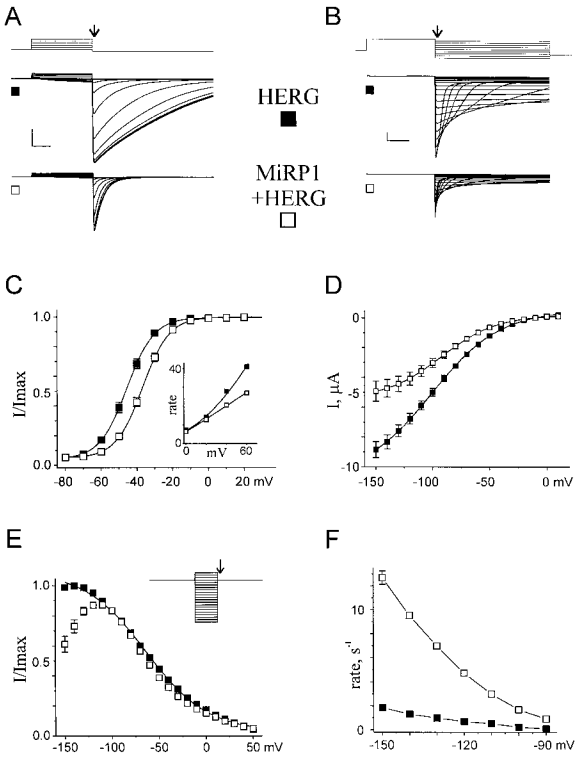

Figure 2. rMiRP1 Is an Ion Channel Subunit

Attributes of channels formed with HERG (filled squares) or rMiRP1 and HERG (open squares) subunits were assessed in whole oocytes with 0.3 mM Ca^{2+}, 100 mM KCl solution by the indicated protocols, as described in Experimental Procedures.

(A) Raw current traces by protocol 1 (inset); scale bars, 1 μA and 1 s.

(B) Raw current traces by protocol 3 (inset), otherwise as in (A).

(C) Steady-state activation by protocol 1; tail currents measured at arrow, mean ± SEM for groups of ten oocytes, normalized to I_{Max} (40 mV). Lines according to the Boltzmann function: $1/\{1 + \exp[(V_{1/2} - V)/V_s]\}$, where $V_{1/2}$ is half-maximal voltage and V_s the slope factor; error bars represent SEM. $V_{1/2}$ was −46 ± 1 and −37 ± 1 mV, and V_s was 11.4 ± 0.2 and 11.7 ± 0.1 for HERG and rMiRP1 + HERG channels, respectively. (C, inset) Activation rates at various voltages by protocol 2, groups of three oocytes, normalized to the rate at 60 mV.

(D) Peak tail currents by protocol 3; fit as in (C); mean ± SEM for groups of ten oocytes; peak at −150 mV for HERG and rMiRP1 + HERG channels was −8.8 ± 0.5 and −4.9 ± 0.7 μA, respectively.

(E) Steady-state inactivation by protocol 4 (inset); mean ± SEM for groups of eight oocytes, normalized to peak (-140 mV).

(F) Deactivation rates at various voltages by protocol 3; current relaxation was fit with a single exponential ($I = Ae^{-t/\tau}$) with groups of eight oocytes; for HERG and rMiRP1 + HERG channels at −120 mV, τ^{-1} was 1.5 ± 0.2 and 0.21 ± 0.01 s, and A was 7.9 ± 0.4, and 4.2 ± 0.5 μA, respectively.

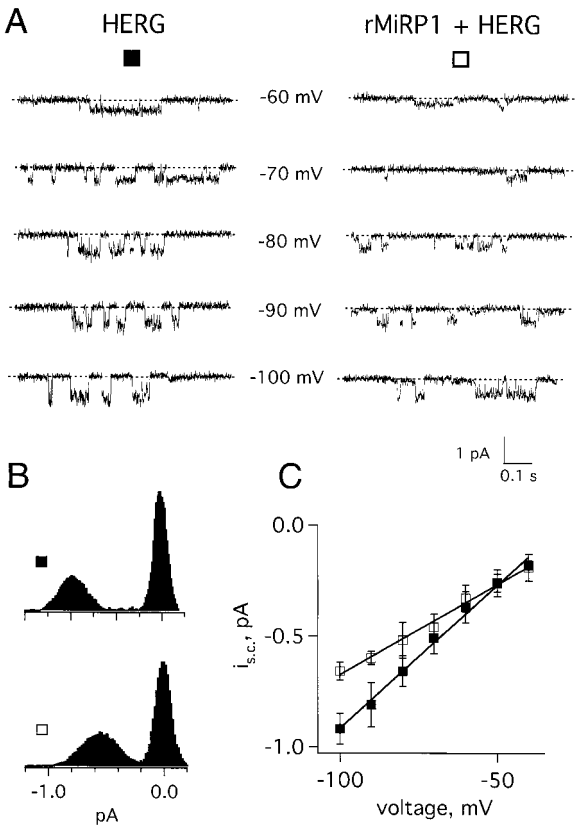

Figure 3. Single rMiRP1/HERG Channels Are Similar in Conductance to Native I_{Kr} Channels, While HERG Channels Are Not

Studies of rMiRP1/HERG channels (open squares) or HERG channels (filled squares) were performed in cell-attached oocyte patches with 0.3 mM Ca^{2+}, 100 mM KCl solution by protocol 7, as described in Experimental Procedures.

(A) Single-channel currents at various voltages; scale bars, 0.5 pA and 0.2 s.

(B) All points histograms computed at −90 mV from the patches in (A) with roughly 30,000 events (150 transitions) recorded prior to deactivation and does not reflect P_o.

(C) Current–voltage relationships for single HERG or rMiRP1 + HERG channels in cell-attached patches (n = 5) held at the indicated voltages; all points histograms were constructed with 1.3×10^5 events at each voltage, ~400 transitions. Slope conductances were 12.9 ± 2.0 and 8.2 ± 1.4 pS, for HERG and rMiRP1 + HERG channels, respectively. Filtered at 0.5 kHz.

HERG channels activate from a closed to open state (C→O) upon depolarization but pass little outward current because they rapidly inactivate (O→I). With repolarization back to negative potentials, channels rapidly recover from the inactive state to the open state (O←I) and pass K^+ current until they close (C←O). The time spent in the open state during repolarization is significant because step *c* is fast compared to step *d* (a transition called deactivation). This is why the rate of deactivation has such a strong influence over the magnitude of K^+ current. Because lower Ca^{2+} concentrations slow the gating transitions of native I_{Kr} and HERG channels (Sanguinetti and Jurkiewicz, 1992; Sanguinetti et al., 1995; Ho et al., 1996, 1998), a 0.3 mM Ca^{2+}, 100 mM KCl solution was initially used to study the influence of rMiRP1 on channel function.

Activation was found to be altered by rMiRP1 using a protocol that estimates the fraction of channels that leave the closed state at equilibrium after the membrane is stepped to various test potentials (Figures 2A and 2C). Channels containing rMiRP1 required a more positive potential, ~9 ± 1 mV (mean ± SEM for ten oocytes), to achieve half-maximal activation ($V_{1/2}$) when compared to channels formed only with HERG subunits; in contrast, no change in the slope factor was apparent (Figure 2C).

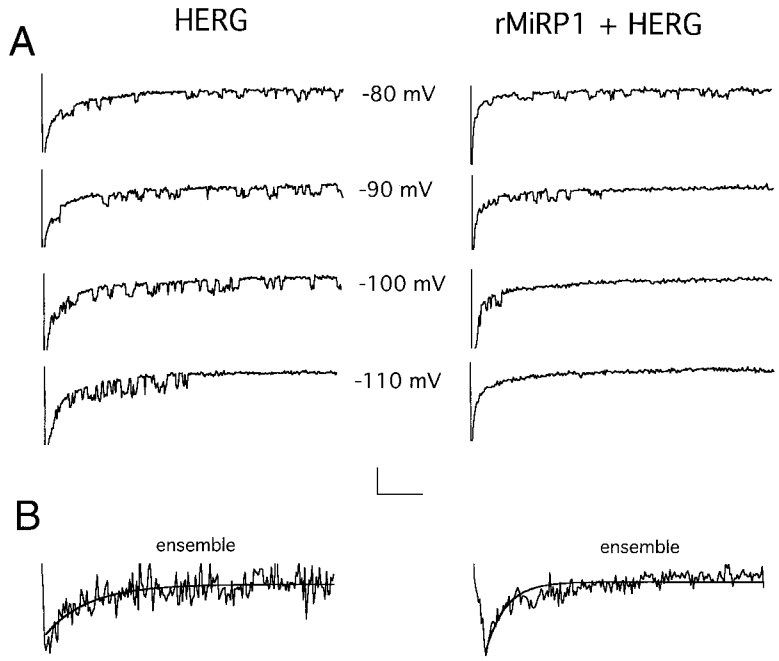

Figure 4. Single rMiRP1/HERG Channels Deactivate More Rapidly Than HERG Channels

(A) Deactivation of single channels in cell-attached patches as in Figure 3; scale bars, 2 pA and 0.75 s.

(B) Ensemble of 50–70 trials performed as in (A) at −100 mV; capacitance transients were neutralized by null trace subtraction. Histograms were fit with a single exponential function ($I = I_o + Ie^{-t/\tau}$); $\tau^{-1} = 300$ ms, $I_o = -8$ pA, and $I = -20$ pA for HERG channels; $\tau^{-1} = 131$ ms, $I_o = -10$ pA, and $I = -24$ pA for channels containing rMiRP1 and HERG subunits. Scale bars, 10 pA and 0.5 s.

This shift in $V_{1/2}$ appeared to result from a slower rate of activation of channels formed with rMiRP1 (Figure 2C inset, model step *a*).

Peak currents were also altered by rMiRP1. The size of whole-cell currents was assessed using a protocol that fully activates channels by sustained depolarization and then measures maximal currents at various test potentials (Figure 2B). Mean peak currents were 40% smaller for channels with rMiRP1 compared to those formed only with HERG subunits (Figure 2D). As shown below, this resulted primarily from altered single-channel current (that is, the number of ions moving through the open channel per unit time) rather than changes in channel gating.

Inactivation (step *b*) was judged using a steady-state protocol (Smith et al., 1996) in which channel inactivation comes to equilibrium at various voltages during a prepulse so brief that little deactivation can occur; then, the fraction of channels in the inactive state is assessed by stepping the voltage to a test potential. Inactivation of HERG channels was the same as those containing rMiRP1 with prepulse voltages from −100 to 30 mV (Figure 2E). The current–voltage relationships diverged only at potentials more negative than −100 mV where differences in deactivation became apparent. Recovery from inactivation (step *c*) remained extremely rapid in both channel types.

Deactivation of channels (step *d*) was markedly altered by rMiRP1. After channels were fully activated by a depolarizing step, the speed with which channels returned to the closed state was assessed at various test potentials. rMiRP1 increased the deactivation rate (Figure 2F). Thus, HERG channels did not deactivate appreciably until −100 mV and required a step 50 mV more negative to achieve the same deactivation rate as channels formed with rMiRP1. While deactivation was voltage sensitive, the rate increase with rMiRP1 was unchanged from −100 to −150 mV (data not shown).

Unitary Conductance and Deactivation of rMiRP1/HERG and Native I_{Kr} Channels Are Similar

Single-channel analysis revealed the primary mechanism by which rMiRP1 decreased peak whole-cell currents (Figure 2D). rMiRP1 caused a decrease in unitary current of ~40% through open channel complexes (Figures 3A and 3B). Thus, single HERG channels were found to have a slope conductance of 12.9 ± 2 pS (Figure 3C), as previously described (Zou et al., 1997). Channels containing rMiRP1 showed a value of 8 ± 1 pS (Figure 3C). This is similar to the unitary conductance value reported for native I_{Kr} channels in rabbit atrioventricular node cells studied under identical conditions (8.4 pS; Shibasaki, 1987).

The increased rate of channel deactivation seen when channels were formed with rMiRP1 and studied in whole-cell mode (Figure 2F) was also apparent at the single-channel level (Figure 4). While single HERG channels remained open for many seconds in patches held at −100 mV, as reported previously (Zou et al., 1997), channels formed with rMiRP1 closed rapidly (Figure 4A). Ensemble averages of 50–70 traces emphasize the 2.3-fold acceleration of deactivation caused by formation of channels with rMiRP1 (Figure 4B). In this way, channels formed with rMiRP1 were again like native I_{Kr} channels. In human and mouse ventricular myocytes, I_{Kr} channels were found to deactivate 2- to 3-fold faster than channels formed with HERG or murine ether a-go-go related gene (MERG) subunits alone (Yang et al., 1994; Sanguinetti et al., 1995; Lees-Miller et al., 1997; London et al., 1997).

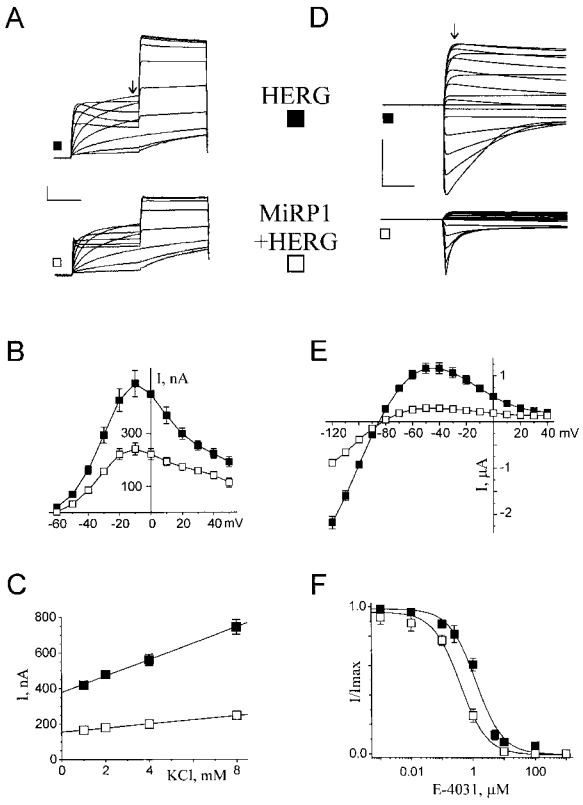

Figure 5. rMiRP1/HERG Channels Are Similar to Native I_{Kr} Channels in Their Regulation by K^+ and Deactivation Rate, While HERG Channels Are Not

Studies of rMiRP1/HERG channels (open squares) or HERG channels (filled squares) were performed in whole oocytes with 1 mM Ca^{2+}, 4 mM KCl solution by protocols as described in Experimental Procedures.

(A) Raw current traces by protocol 6; scale bars, 0.1 μA and 1 s.

(B) Current–voltage relationship at end of the activating pulse (arrow); mean ± SEM for groups of seven oocytes; studied as in (A).

(C) Variation of current amplitude with external KCl; mean ± SEM for groups of eight cells studied as in (A) at 0 mV. Solid lines are linear fits to the data; for HERG, the relation gives a slope of 46 ± 2 and intercept of 377 ± 6 nA (R = 0.998); for rMiRP1/HERG, slope = 11.7 ± 0.4 and intercept = 155 ± 2 nA (R = 0.999).

(D) Raw current traces by protocol 3; 1 s prepulse and test pulse durations; scale bars, 1 μA and 250 ms.

(E) Current–voltage relationship at peak (arrow in [D]); mean ± SEM for groups of five oocytes; at −50 mV currents were 1200 ± 100 and 300 ± 60 nA, while at −120 mV they were −2200 ± 100 and −900 ± 70 for HERG and rMiRP1/HERG channels, respectively.

(F) Steady-state block by various concentrations of E-4031 in 20 KCl solution assessed by protocol 5 and plotted as the fraction of unblocked current for groups of six oocytes; inhibition constants are reported in the text. Neither channel type showed block with the initial pulse.

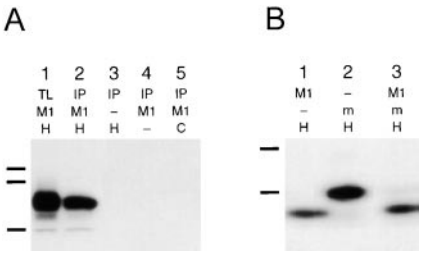

Figure 6. rMiRP1 and HERG Subunits Form Stable Complexes

(A) Expression in COS cells of rMiRP1-HA (M1), HERG-cmyc (H), and connexin43-cmyc (C). Lanes contain total cell lysate (TL) or immunoprecipitations (IP) performed with anti-cmyc antibody. SDS–PAGE (10%–16%) and Western blot visualization with anti-HA antibody. Cells were transfected with subunits as follows: lanes 1 and 2, M1 + H; lane 3, H; lane 4, M1; lane 5, M1 + C; bars mark 32.7, 30.2, and 24 kDa.

(B) rMiRP1 forms complexes with HERG in preference to MinK in vitro. Lanes contain immunoprecipitates using anti-cmyc antibody of ^{35}S-methionine labeled translation products generated with rabbit reticulocyte lysate and were visualized by autoradiography. Reaction mixtures contained subunits rMiRP1 (M1), rMinK (m), and HERG-cmyc (H) as follows: lane 1, M1 + H; lane 2, m + H; lane 3, M1 + m + H; scale bars, 30.2 and 24 kDa.

Regulation by External K^+ of rMiRP/HERG and Native I_{Kr} Channels Is Similar

Ionic conditions like those in human plasma (1 mM ionized Ca^{2+}, 4 mM KCl solution) were next employed. One hallmark of native I_{Kr} channels and those formed only of HERG subunits is a negative slope for the current–voltage relationship at depolarized voltages; this results from channel inactivation (Sanguinetti et al., 1995; Smith et al., 1996; Spector et al., 1996b). As expected, rMiRP1 had no significant effect on the shape of the current–voltage relationship (Figures 5A and 5B), since it had not altered channel inactivation (Figure 2E). In contrast, upregulation of outward K^+ currents associated with elevation of external K^+ concentration, another notable feature of both native I_{Kr} and HERG channels (Sanguinetti and Jurkiewicz, 1992; Sanguinetti et al., 1995), was modified by rMiRP1. Channels containing rMiRP1 were less responsive than HERG channels when external K^+ ion was varied from 1 to 8 mM (Figure 5C). A shallow response to external K^+, like that seen here with rMiRP1, was also found when native I_{Kr} channels were studied in murine atrial cells or guinea pig ventricular myocytes (Shibasaki, 1987; Scamps and Carmeliet, 1989; Sanguinetti and Jurkiewicz, 1992; Sanguinetti et al., 1995; Yang and Roden, 1996). Studied in plasma-like ionic conditions and whole-cell mode, rMiRP1 was again observed to increase the rate of deactivation, ~2-fold from $\tau = 130 \pm 8$ ms for HERG channels to 61 ± 4 ms (mean ± SEM, protocol 3, n = 5 cells) (Figure 5D).

The combined effects of rMiRP1 on activation, deactivation, and regulation by external K^+ ion, under these ionic conditions, produced a current–voltage relationship that was little changed in its shape compared to channels formed by HERG subunits alone (Figure 5B). However, oocytes expressing channels with rMiRP1 passed half the inward current and one-quarter of the outward current of those with HERG channels (Figures 5D and 5E).

Stable Association of rMiRP1 and HERG Subunits

Subunit interaction between rMiRP and HERG was evaluated first by studying the proteins modified with epitope tags and expressed in mammalian tissue culture cells. Epitopes had no apparent effect on macroscopic channel activity (data not shown). Transient expression of rMiRP1-HA in COS cells, followed by Western blot analysis with anti-HA antibody, revealed three specific

Table 1. Activation and Deactivation Parameters of hMiRP1/HERG Channels and Channels Formed Only with HERG Subunits

Channel (No. of Cells)	Activation $V_{1/2}$ (mV)	Activation slope (mV)	Deactivation τ_f (s)	Deactivation τ_s (s)	Deactivation Ratio $I_f/(I_s + I_f)$
HERG (11)	−25 ± 5	9.1 ± 1.4	241 ± 119	782 ± 376	0.59 ± 0.19
WT hMiRP1 (21)	−21 ± 6	9.5 ± 1.0	80 ± 26	483 ± 491	0.82 ± 0.03
T8A hMiRP1 (15)	−29 ± 6	9.4 ± 1.7	100 ± 40	590 ± 370	0.83 ± 0.05
Q9E hMiRP1 (14)	−12 ± 4	7.6 ± 0.4	100 ± 27	750 ± 451	0.80 ± 0.11
M54T hMiRP1 (10)	−21 ± 6	7.2 ± 2.0	37 ± 8	266 ± 35	0.81 ± 0.06

Activation kinetics were estimated in whole CHO cells in 1.0 mM Ca^{2+}, 4 mM KCl solution (Experimental Procedures). Currents were measured and fitted for activation parameters as in Figure 8; for deactivation, a double exponential function ($I_0 + I_f e^{(-t/\tau_f)} + I_s e^{(-t/\tau_s)}$) and protocol 7 were used (−120 mV). When blockade was studied in 1 mM Ca^{2+}, 1 mM KCl solution, channels with wild-type hMiRP1 showed a $V_{1/2} = -20 \pm 5$ mV and slope = 9.2 ± 2, while Q9E-hMiRP1 channels had a $V_{1/2} = -12 \pm 5$ mV and slope = 7.6 ± 1 (n = 7–13 cells).

bands at migration distances appropriate for the mature protein and small amounts of its mono- and unglycosylated forms (Figure 6A, lane 1); endoglycosidase F treatment resulted in collapse of the profile to one specific band at the lowest predicted mass (data not shown).

Coexpression of rMiRP1-HA with HERG-cmyc allowed recovery of rMiRP1-HA by immunoprecipitation (IP) with an anti-cmyc monoclonal antibody (Figure 6A, lane 2). Recovery was shown to be specific because anti-cmyc IP gave no signal when HERG-cmyc was expressed alone (Figure 6A, lane 3), when rMiRP1-HA was expressed alone (Figure 6A, lane 4), or when the channel protein connexin 43-cmyc was expressed with rMiRP1-HA (Figure 6A, lane 5).

As reported previously, MinK and HERG-cmyc also coassemble (McDonald et al., 1997). To compare the binding of MinK and MiRP1 to HERG-cmyc, an assay was performed using ^{35}S-labeled MinK and MiRP1 subunits synthesized in vitro. Incubation of rMiRP1 and HERG-cmyc followed by anti-cmyc IP allowed strong recovery of rMiRP1, as judged by autoradiography (Figure 6B, lane 1). Similarly, incubation of rMinK and HERG-cmyc allowed strong recovery of rMinK (Figure 6B, lane 2). When rMiRP1 and rMinK were mixed in a 1:1 ratio and incubated at 5-fold molar excess with HERG-cmyc, anti-cmyc IP led to strong recovery of rMiRP1, like that seen in the absence of rMinK, while recovery of rMinK was poor (Figure 6B, lane 3). Thus, rMinK and rMiRP1 could each assemble with HERG-cmyc. However, under these in vitro conditions, the presence of both peptides favored formation of stable rMiRP1/HERG complexes in preference to those with rMinK.

Cloning and Function of the Human MiRP1 Gene *hKCNE2*

Based on the presumed molecular correlation of MiRP1/HERG channel complexes and native cardiac I_{Kr} channels, we cloned the gene for human MiRP1 (*hKCNE2*) to screen for the presence of mutations in patients with cardiac arrhythmias. Multiple identical clones were isolated from a human cardiac muscle cDNA library (Experimental Procedures). As in rat, transcripts were detected in heart and skeletal muscle (data not shown). The human cDNA also predicted a protein of 123 amino acids with two N-linked glycosylation sites, a single transmembrane segment, and two protein kinase C–mediated phosphorylation sites. Alignment of rat and human MiRP1 showed 82% identity and 97% homology (Figure 1C).

The *hKCNE2* gene was localized to chromosome 21q22.1 (accession number AP000052). This was notable because *hKCNE1*, the gene encoding MinK, was previously localized to this site (accession number AP000053). The two genes are arrayed in opposite orientation, separated by 79 kb. Their open reading frames share 34% identity, and both are contained in a single exon (Splawski et al., 1998). This suggests that MiRP1 and MinK are related through gene duplication and divergent evolution.

Wild-type human MiRP1, studied by transient expression in Chinese hamster ovary (CHO) cells using 1 mM Ca^{2+}, 4 mM KCl solution, had the same effects as rat MiRP1. Like channels with rMiRP1, hMiRP1/HERG complexes required depolarization to more positive potentials to achieve half-maximal activation and showed no change in slope factor compared to channels formed by HERG subunits alone (Table 1). Like rMiRP1, hMiRP1 did not alter steady-state inactivation (data not shown). Like those with rMiRP1, hMiRP1/HERG complexes deactivated ~3-fold faster than HERG channels (Table 1, τ_f at −120 mV). Finally, the unitary conductance of channels formed with hMiRP1 (in oocytes) was the same (8.0 ± 0.7 pS) as that measured for channels with rMiRP1 (n = 11 patches, data not shown, as in Figure 3C).

hMiRP1/HERG and Native I_{Kr} Channels Exhibit Biphasic Class III Block Kinetics

A fundamental discrepancy between cloned HERG and native I_{Kr} channels is their disparate responses to methanesulfonanilide class III antiarrhythmics like E-4031. Closed HERG channels exposed to the agents show little inhibition with an initial test pulse and achieve equilibrium blockade slowly with repetitive activating pulses or prolonged depolarization (Spector et al., 1996b; Zhou et al., 1998). In contrast, native I_{Kr} channels show two phases of blockade: significant inhibition with the initial test pulse and ready relaxation to equilibrium block with subsequent test pulses (Carmeliet, 1992, 1993).

As expected, HERG channels expressed in CHO cells and bathed in E-4031 showed minimal inhibition on the first test pulse (Figure 7A). In marked contrast, channels formed with hMiRP1 were significantly inhibited on the first pulse, like native I_{Kr} channels (Figure 7B). The fraction of unblocked current in the first pulse by 1 μM E-4031 was 0.9 ± 0.1 for HERG channels and 0.6 ± 0.2 for channels formed with MiRP1 and HERG (n = 9 cells).

HERG channels in CHO cells reached equilibrium slowly with repetitive pulses (Figure 7C); relaxation was

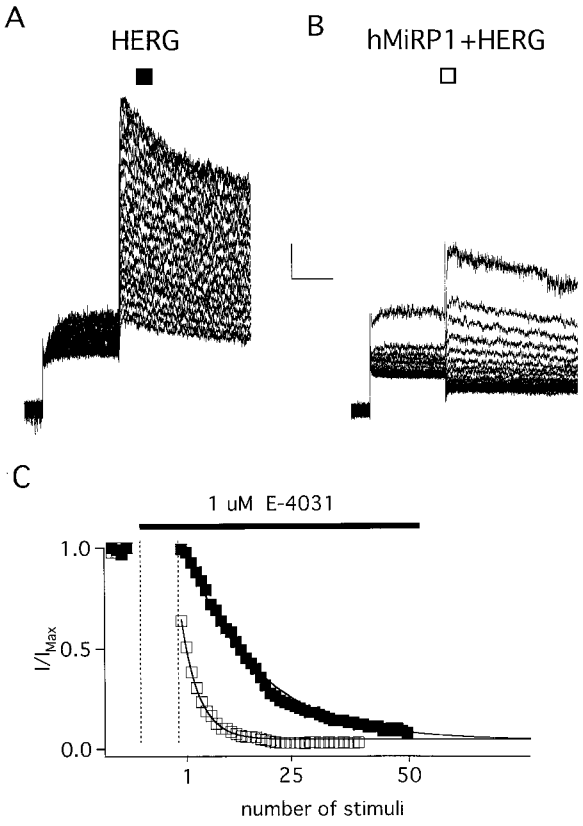

Figure 7. Channels Formed with hMiRP1 and HERG (but Not Those with HERG Alone) Are Blocked by E-4031 with Biphasic Kinetics

CHO cells expressing channel subunits as indicated were stepped from −80 mV to +20 mV for 1 s and then to −40 mV for 2 s with a 0.5 s intercycle interval. Cells were studied for four cycles before drug application, held closed at −80 mV for 1 min in the presence of 1 μM E-4031 (bar), and then studied for 30–70 cycles in the continued presence of the drug.

(A) The first 20 current traces for a cell expressing HERG channels; fraction of unblocked current in the first pulse for this cell was 0.99.

(B) The first 20 current traces for a cell expressing hMiRP1/HERG channels; fraction of unblocked current in the first pulse for this cell was 0.64.

(C) Relaxation to equilibrium blockade for the cells in (A) (HERG channels, filled squares, $\tau = 38$ cycles) and (B) (hMiRP1/HERG channels, open squares, $\tau = 4$ cycles).

best approximated by a single exponential decay with a time constant (τ) of 26 ± 9 pulse cycles (n = 9 cells). Block of channels with hMiRP1 was best described as an initial fast block followed by a single exponential decay with $\tau = 4 \pm 1$ pulse cycles (n = 7 cells, Figure 7C). Thus, mixed channel complexes reproduced the characteristic biphasic blocking kinetics observed with native I_{Kr} channels (Carmeliet, 1992, 1993).

Methanesulfonanilide potency varies widely with cell type and ionic condition (Snyders and Chaudhary, 1996; Yang and Roden, 1996; Yang et al., 1997). Others have found block of HERG channels by E-4031 to be weak in oocytes ($K_i = 588$ nM; Trudeau et al., 1995) and strong in mammalian tissue culture cells ($K_i = 7.7$ nM; Zhou et al., 1998). In oocytes, we also find E-4031 block of HERG channels to be poor ($K_i = 1{,}250 \pm 200$ nM); channels formed with rMiRP1 and HERG were ~3-fold more sensitive ($K_i = 380 \pm 60$) (Figure 5F). In CHO cells, HERG channels were strongly blocked by E-4031 ($K_i = 8.8 \pm 0.8$ nM); again, channels formed with hMiRP1 were ~2-fold more sensitive ($K_i = 4.6 \pm 0.6$ nM; n = 6 cells). Native I_{Kr} channels in ferret cardiac myocytes were found to be sensitive to E-4031 ($K_i = 10.3$ nM; Liu et al., 1996).

Mutations in Human MiRP1 Are Associated with Arrhythmia

To test the hypothesis that MiRP1 mutants cause cardiac arrhythmia, we screened a panel of 20 patients with drug-induced arrhythmia and 230 patients with inherited or sporadic arrhythmias and no mutations in their *KVLQT1*, *HERG*, *SCN5A*, or *KCNE1* genes. A control population of 1010 individuals was also evaluated. Analysis by SSCP and DNA sequencing revealed three abnormalities and one polymorphism.

Q9E-hMiRP1

One of 20 patients with drug-induced arrhythmia had a C to G transversion at nucleotide +25 of *hKCNE2*, producing a Q9 to E substitution in the putative extracellular domain of hMiRP1. This mutation was not identified in 1010 control individuals. The patient is a 76-year-old African American female with a history of high blood pressure, non–insulin-dependent diabetes, and stroke. Two baseline electrocardiograms showed QT intervals corrected for heart rate that were borderline prolonged (QTc = 460 ms). Echocardiography revealed concentric left ventricular hypertrophy with mild to moderate diffuse hypokinesis but no ventricular dilatation. The patient was admitted to the hospital with pneumonia and treated with seven doses of intravenous erythromycin, 500 mg every 6 hr, and then switched to oral clarithromycin, 500 mg every 12 hr. After two doses of clarithromycin, electrocardiography showed a QTc of 540 ms. The patient developed TdP and VF, requiring defibrillation. At the time, she was hypokalemic with a serum potassium level of 2.8 meq/l.

M54T-hMiRP1

One of 230 patients with inherited or sporadic arrhythmias had a T to C transition at nucleotide +161, causing substitution of M54 for T in the predicted transmembrane segment. This mutation was not identified in 1010 control individuals. This patient is a 38-year-old Caucasian female who was in good health. She was on no medications. This individual had VF while jogging. Her resuscitation required defibrillation. The results from echocardiography and cardiac catheterization with electrophysiologic studies and right ventricular biopsy were normal. Subsequent electrocardiograms showed an atypical response to exercise with QTc intervals ranging from 390 to 500 ms. An automatic internal defibrillator was placed.

I57T-hMiRP1

Another of the 230 patients with inherited or sporadic arrhythmias had a T to C transition at +170, causing an I57 to T substitution in the predicted transmembrane segment. This patient is a 48-year-old Hispanic female who is in good health and has no history of TdP or VF. Her resting electrocardiogram shows a prolonged QT interval (QTc = 470 ms). She is a member of a multigenerational family now under genetic, clinical, and biophysical evaluation.

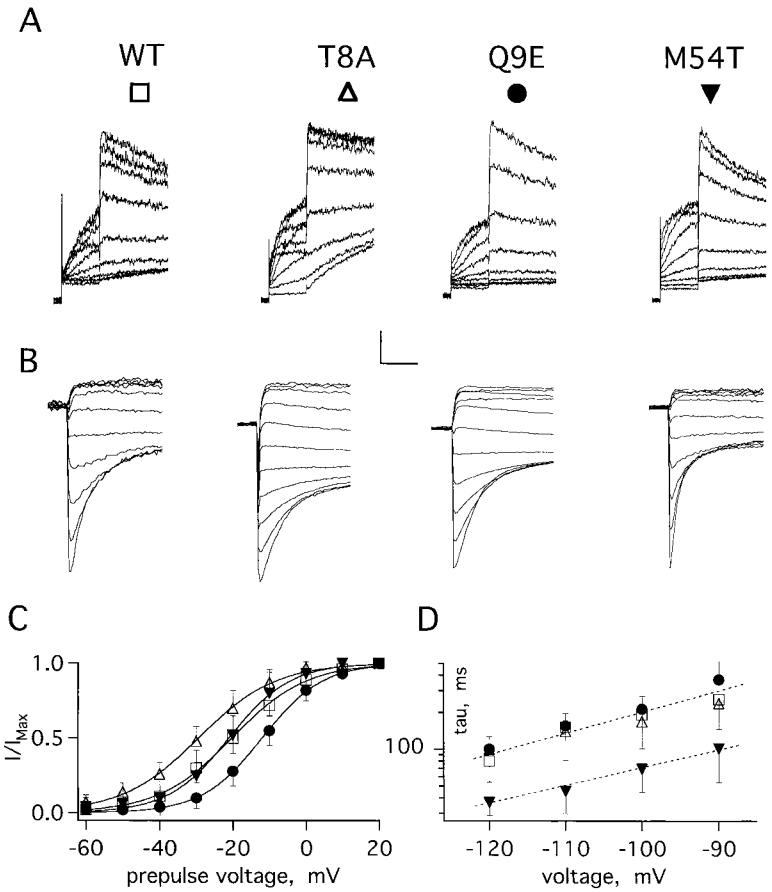

Figure 8. Function of Channels with Wild-Type or Arrhythmia-Associated hMiRP1 Subunits

(A) Raw current traces with wild type (WT), T8A, Q9E or M54T-hMiRP1 and HERG in whole CHO cells by protocol 6 with 1 mM Ca^{2+}, 4 mM KCl solution (Experimental Procedures); scale bars represent 15 pA for WT; 50 pA for T8A, Q9E, and M54T-hMiRP; and 0.5 s.

(B) Tail currents elicited by depolarizing to 20 mV (data not shown) and repolarizing to voltages from −20 to −120 mV, otherwise as in (A); scale bars represent 50 pA for WT, 100 pA for T8A and M54T, 500 pA for Q9E-hMiRP1, and 0.1 s.

(C) Activation: isochronal Po curves for WT (open squares), T8A (open triangles), Q9E (filled circles), and M54T-hMiRP1 (filled triangles); curves are mean ± SEM for groups of 10–14 cells and are fit as in Figure 2C; half-maximal activation voltage and slope factors are reported in Table 1.

(D) Deactivation: fast component, for WT (open squares), T8A (open triangles), Q9E (filled circles), and M54T-hMiRP1 (filled triangles); values for fast and slow rates and their weights were estimated by fitting raw current traces to a double exponential function (Table 1).

T8A-hMiRP1

In 18 out of 1260 individuals screened, an A to G polymorphism at nucleotide +22 produced a T8 to A change in the putative extracellular domain of MiRP1. The change was found in 1 patient with quinidine-induced arrhythmia, 1 with inherited or sporadic arrhythmia, and 16 controls.

Arrhythmia-Associated hMiRP1 Mutants Decrease K^+ Flux

Wild-type hMiRP1/HERG channels and those formed with Q9E, M54T, I57T, or T8A-hMiRP1 were compared by transient expression in CHO cells using 1 mM Ca^{2+}, 4 mM KCl solution. Mutant channels formed with Q9E-hMiRP1 and HERG were like those formed with wild-type subunits in their steady-state inactivation and rate of deactivation (Figures 8B and 8D; Table 1). However, this mutant increased the voltage dependence of channel activation. Thus, Q9E-hMiRP1 channels required depolarization to more positive potentials to achieve half-maximal activation and had a diminished slope factor compared to wild type (Figure 8C and Table 1). An increase in voltage dependence yields fewer open channels for a given depolarizing step and, therefore, decreased K^+ flux. In the heart, diminished K^+ current is predicted to slow phase 3 repolarization. This lengthens the cardiac action potential duration and is reflected on the surface electrocardiogram as a prolonged QT interval.

Mutant channels formed with M54T-hMiRP1 were like wild type in their steady-state inactivation (data not shown). However, this mutant also increased the voltage dependence of activation, in this case by diminishing the activation slope factor without altering $V_{1/2}$ (Figure 8C and Table 1). In addition, channels formed with this mutant showed a speeded rate of closing; these channels deactivated ~3-fold faster than those with wild-type hMiRP1 and 6- to 7-fold faster than channels formed by HERG subunits alone (Figure 8D and Table 1). As before, increased voltage dependence results in fewer open channels for a given voltage step; faster deactivation indicates that mutant channels, if they do open, will close more rapidly than wild type. In the heart, both these effects would reduce K^+ current, prolonging the cardiac action potential and the QT interval measured on an electrocardiogram.

I57T-hMiRP1 also diminished K^+ flux through MiRP1/HERG channel complexes and will be considered in detail elsewhere.

The T8A-hMiRP1 variant was isolated from 18 of 1260 individuals screened. While channels containing the variant were similar to those with wild-type MiRP1, they showed decreased voltage dependence for activation, opening more readily upon depolarization (Figures

8B–8D and Table 1). The variant was found in two patients with arrhythmia, one with quinidine-induced QT prolongation (500 ms). Because quinidine is known to inhibit cardiac I_{Kr} channels (Roden et al., 1986), we compared blockade of channels formed with wild-type or T8A-hMiRP1. Quinidine sensitivity of the two channel types was not significantly different; wild-type channels exhibited an equilibrium constant (K_i) of 0.79 ± 0.18 μM, while T8A-hMiRP1 channels had a K_i = 0.84 ± 0.10 μM with Hill coefficients of 1.1 ± 0.07 and 1.0 ± 0.05, respectively (n = 7 cells, protocol 1 at −40 mV).

Increased Blockade by Clarithromycin of Channels Formed with Q9E-hMiRP1

Q9E-hMiRP1, associated with clarithromycin-induced TdP and VF, assembles with HERG to form channels with increased sensitivity to blockade by this macrolide antibiotic. The dose leading to half block of peak outward current for channels formed with wild-type hMiRP1 was 0.72 ± 0.18 mM, similar to that measured for channels formed only with HERG (0.75 ± 0.31 mM). In contrast, channels formed with Q9E-hMiRP1 exhibited a K_i of 0.24 ± 0.04 mM (Figures 9A and 9B). Blockade was observed only at voltages positive to the threshold for activation and increased as the prepulse potential became more positive (Figure 9C). This is consistent with block of open channels, a mechanism thought to underlie inhibition of I_{Kr} channels by class III antiarrhythmic agents (Spector et al., 1996a; Wang et al., 1997b). However, clarithromycin also caused a 10 mV shift to more positive potentials in the $V_{1/2}$ (with no change in slope factor) for both wild-type and Q9E-hMiRP1 channels (Figure 9C). At present, the mechanism of clarithromycin inhibition is best described as state dependent.

As native I_{Kr} channels show increasing sensitivity to class III agents with lowered external K^+ (Yang and Roden, 1996), we reassessed clarithromycin block when bath K^+ concentration was reduced from 4 to 1 mM. While changing the solution had no effect on activation of either channel (Table 1), the blocking potency of clarithromycin was increased ~20% for both channels formed with wild-type MiRP1 and those with Q9E-hMiRP1 (wild-type K_i = 0.59 ± 0.1, for Q9E-hMiRP1 K_i = 0.20 ± 0.07 mM, n = 6 cells each, data not shown). Thus, channels formed with Q9E-hMiRP1 are more sensitive to clarithromycin blockade, and inhibition is intensified by intercurrent hypokalemia.

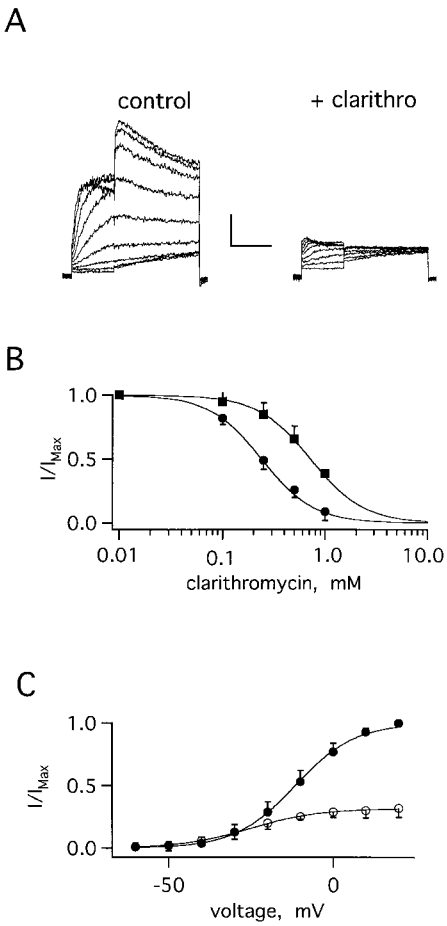

Figure 9. Q9E-hMiRP1 Is Associated with Clarithromycin-Induced Arrhythmia and Increased Drug Sensitivity

Unless indicated, 1 mM Ca^{2+}, 4 mM KCl solution (Experimental Procedures) was used.

(A) Raw current traces of Q9E-hMiRP1 expressed with HERG in CHO cells by protocol 6; scale bars, 0.1 pA and 0.1 s.

(B) Variation of peak tail current amplitude at equilibrium with varying doses of clarithromycin after activation at +20 mV; half-maximal blocking concentrations are in the text; Hill coefficients were 1.7 ± 0.2 and 1.7 ± 0.1 for WT (open squares) and Q9E-hMiRP1 (open circles), respectively.

(C) Current–voltage relationship as in (A), mean ± SEM for groups of six cells in the absence (filled circles) or presence (open circles) of 0.5 mM clarithromycin. Data were fitted using the Boltzman equation in Figure 2C and multiplied by the reciprocal of the fraction of unblocked current; with 0.5 mM clarithromycin the $V_{1/2}$ for wild type was −30 ± 8 mV (data not shown), while it was −25 ± 5 mV for Q9E-hMiRP1 (shown); slope factors were unchanged. In 1 mM Ca^{2+}, 1 mM KCl solution and 0.5 mM clarithromycin (data not shown), the $V_{1/2}$ for wild type was −32 ± 6 mV and for Q9E-hMiRP1 was −29 ± 10 mV; slope factors were again unchanged.

Discussion

The *KCNE* Peptides: An Emerging Superfamily Required for Normal Ion Channel Function

MinK, encoded by *KCNE1*, has 129 amino acids, a single transmembrane segment, and is expressed in numerous tissues (Takumi et al., 1988; Kaczmarek and Blumenthal, 1997). Inherited mutations of MinK are associated with LQTS and congenital deafness (Schulze-Bahr et al., 1997; Splawski et al., 1997; Tyson et al., 1997; Duggal et al., 1998). The molecular basis for these disturbances is understood: I_{Ks} channels, essential to normal function of the heart and auditory system, are coassemblies of MinK and KvLQT1, a pore-forming subunit (Sanguinetti et al., 1996b; Vetter et al., 1996). While channels containing only KvLQT1 subunits can function in experimental cells, I_{Ks} channels have slower activation and deactivation kinetics, larger single-channel conductance, higher affinity for class III antiarrhythmics, and greater sensitivity to second messengers (Sanguinetti et al., 1996b; Busch et al., 1997; Kaczmarek and Blumenthal, 1997; Sesti and Goldstein, 1998; Yang and Sigworth,

1998). These properties are due to intimate physical association of MinK and KvLQT1 subunits (Goldstein and Miller, 1991; Wang et al., 1996; Tai et al., 1997; Sesti and Goldstein, 1998; Tai and Goldstein, 1998). Despite its functional and clinical significance, this type of mixed complex was thought uncommon, as MinK homologs, or subunits subserving a similar function, had been unknown.

Here, we have delineated the chromosomal location, cDNA sequence and predicted product, wild-type behavior, and arrhythmia association of a gene homologous to *KCNE1* (MinK). MiRP1, encoded by *KCNE2*, has 123 amino acids, a single predicted transmembrane segment, and is expressed in cardiac and skeletal muscle. Like MinK, MiRP1 coassembles with a pore-forming subunit to create stable complexes whose functional attributes resemble those of a native cardiac potassium channel. While MinK/KvLQT1 complexes recreate the behaviors of I_{Ks} channels, MiRP1/HERG complexes recapitulate those of I_{Kr} channels. Compared to channels formed by HERG subunits alone, those containing MiRP1 show altered voltage-dependent activation, kinetics of deactivation, unitary conductance, sensitivity to regulation by external K^+, and pharmacology. In mutant form, MiRP1 is associated with inherited and acquired cardiac arrhythmia. MinK and MiRP1 are revealed to be essential for normal cardiac ion channel function.

The variety of channel assemblies that incorporate *KCNE* peptides in native cells and the factors governing complex formation remain to be determined. Functional specificity is inferred from the absence of effects when rMiRP1 was coexpressed with seven different K^+ channel subunits in oocytes (Results). Specific binding is indicated by the preferential association of MiRP1 rather than MinK with HERG in vitro (Figure 6), even though MinK/HERG assemblies can form (Figure 6; McDonald et al., 1997). However, in vitro findings do not clarify the mechanisms by which complex formation is regulated in vivo. While a role for *KCNE* peptides in channels other than I_{Kr} and I_{Ks} seems probable, studies of human and mouse MiRP2 (*KCNE3*) and mouse MiRP3 (*KCNE4*) have indicated only that they do not alter HERG or KvLQT1 currents or activate channel subunits endogenous to oocytes.

MiRP1/HERG Complexes Function like Native Cardiac I_{Kr} Channels

Channels formed only with HERG subunits are known to differ from native I_{Kr} channels in gating, conductance, regulation by K^+, and block by methanesulfonanilides (Shibasaki, 1987; Sanguinetti and Jurkiewicz, 1992; Yang et al., 1994; Sanguinetti et al., 1995; Trudeau et al., 1995; Veldkamp et al., 1995; Ho et al., 1996, 1998; Howarth et al., 1996; Spector et al., 1996a; Zou et al., 1997). The idea that native I_{Kr} channels are formed by coassembly of MiRP1 and HERG subunits is consistent with six observations reported here.

First, the single-channel conductance of channels containing MiRP1 is smaller than that of HERG channels but the same as that of I_{Kr} channels in isolated rabbit and human cardiocytes (Shibasaki, 1987; Veldkamp et al., 1995; Zou et al., 1997). Second, MiRP1/HERG complexes and I_{Kr} channels in murine and human cardiac myocytes deactivate 3-fold more rapidly than channels formed only of HERG subunits (Yang et al., 1994; Sanguinetti et al., 1995; London et al., 1997; Wang et al., 1997a). Third, MiRP1/HERG complexes, like I_{Kr} channels in murine atrial and guinea pig ventricular myocytes, are less sensitive to regulation by external K^+ than HERG channels (Shibasaki, 1987; Scamps and Carmeliet, 1989; Sanguinetti and Jurkiewicz, 1992; Sanguinetti et al., 1995; Yang and Roden, 1996; Yang et al., 1997). Fourth, MiRP1 and HERG subunits coassemble in a stable fashion. Fifth, a hallmark of native I_{Kr} channels is that blockade by methanesulfonanilide class III antiarrhythmics proceeds in two phases, a fast phase seen with the first test pulse and a slow phase (Carmeliet, 1992). Conversely, HERG channels require repetitive pulsing to voltages positive to the threshold for activation before significant blockade develops (Spector et al., 1996a). Like native I_{Kr} channels in cardiac myocytes, channels formed by assembly of hMiRP1 and HERG show biphasic E-4031 blockade; mixed complexes are significantly inhibited with the first test pulse and slowly relax to equilibrium blockade (Figures 7B and 7C), while channels formed by HERG subunits alone are inhibited only after repetitive test pulses (Figure 7A). Finally, Q9E-hMiRP1 increases clarithromycin sensitivity of MiRP1/HERG channels in vitro (Figure 9). Clarithromycin is known to block I_{Kr} currents in isolated guinea pig and canine ventricular myocytes and, at high doses, to induce a prolonged QT interval and TdP in humans (Daleau et al., 1995; Antzelevitch et al., 1996). That the mutant was isolated from a patient with clarithromycin-induced TdP and VF supports the thesis that native cardiac I_{Kr} channels are formed with hMiRP1.

hKCNE2 Is an Arrhythmia Susceptibility Gene

Molecular genetic data supporting the hypothesis that mutations in the gene for MiRP1 predispose to arrhythmia include identification of three missense mutations associated with LQTS and/or VF. Q9E-hMiRP1 was identified in 1 of 20 individuals with drug-induced arrhythmia. M54T-hMiRP1 and I57T-hMiRP1 were each isolated in 1 of 230 individuals with inherited or sporadic arrhythmias. The alternative explanation, that these are common polymorphisms, has been disproved. Nongenetic data supporting the hypothesis include the observations that I_{Kr} dysfunction is known to cause LQTS and arrhythmia susceptibility, that MiRP1 and HERG coassemble to form I_{Kr}-like channels, and that arrhythmia-associated mutations in *KCNE2* have deleterious effects on channels formed in vitro.

MinK and MiRP1 mutants associated with arrhythmia have common effects. Four mutants of MinK have been associated with inherited LQTS: T7I, D76N, S74L, and TL58,59PP (Schulze-Bahr et al., 1997; Splawski et al., 1997; Tyson et al., 1997; Duggal et al., 1998). Formation of I_{Ks} channels with S74L and/or D76N-MinK decreases K^+ flux (and prolongs the cardiac action potential) by shifting $V_{1/2}$ for activation to more depolarized voltages, speeding deactivation (Splawski et al., 1997; Sesti and Goldstein, 1998) and decreasing single-channel conductance (Sesti and Goldstein, 1998). In a similar fashion, MiRP1 mutants associated with prolongation of the

QT interval decrease K^+ current by increasing the voltage dependence of activation and speeding deactivation. Currents through channels formed with Q9E-hMiRP1 are further reduced compared to wild type when exposed to clarithromycin as they are more sensitive to drug blockade (Figure 9).

Arrhythmia-associated mutations in MiRP1, MinK, HERG, and KvLQT1 produce changes in channel function of similar magnitude. Q9E-hMiRP1 impedes activation and increases sensitivity to macrolide antibiotics (causing a 60% reduction in current relative to wild type at 0 mV with 0.5 mM clarithromycin). M54T-hMiRP1 forms I_{Kr} channels that deactivate twice as fast as wild type, showing a 54% reduction in τ_{fast} (Table 1). Similarly, loss-of-function mutations in HERG and KvLQT1 caused 50%–80% reduction in peak currents (Sanguinetti et al., 1996a; Wollnik et al., 1997), while other LQTS-associated HERG mutants increased deactivation rates by reducing τ_{fast} from 49%–84% (Chen et al., 1999). S74L and D76N-MinK mutations associated with LQTS form I_{Ks} channels with 40%–70% reduced single channel conductance and deactivation rates that are 33%–75% faster (Sesti and Goldstein, 1998). Conversely, T8A-hMiRP1 was not disease associated and functioned like wild type except for a negative shift of 8 mV in the $V_{1/2}$ for activation. This is not expected to cause arrhythmia, as the allele should enhance the capacity of I_{Kr} channels to achieve myocardial repolarization.

The occurrence of TdP during treatment with medications that prolong the cardiac action potential is unpredictable. TdP is a recognized risk of treatment with various antiarrhythmic agents, including quinidine, sotalol and ibutilide, the antihistamine terfenadine, the gastrointestinal prokinetic agent cisapride (Roden, 1998), and the macrolide antibiotics erythromycin (Daleau et al., 1995; Antzelevitch et al., 1996; Drici et al., 1998) and clarithromycin (Lee et al., 1998). In each case, the agents diminish cardiac K^+ currents, in some cases by inhibition of I_{Kr} channels. Baseline characteristics that identify patients at risk for drug-induced TdP include inherited prolongation of QT interval, hypokalemia, female gender, and slow heart rate, each of which prolongs the action potential duration; these observations led Roden (1998) to develop the concept of a "repolarization reserve," that is, excess capacity of the myocardium to effect orderly and rapid repolarization via normal mechanisms. Risk factors for TdP reduce this reserve and make the precipitation of arrhythmia by further stressors more likely.

Thus, a plausible scenario for a prolonged QT interval at baseline in the patient carrying Q9E-hMiRP1 is formation of channels that activate less readily and, therefore, pass less K^+ to accomplish repolarization in a timely fashion. Three additional factors leading to decreased K^+ current may have predisposed this patient to TdP and VF. First, clarithromycin blocks cardiac I_{Kr} channels; this effect would be more pronounced in the patient as Q9E-hMiRP1 channels are 3-fold more sensitive to the drug. Second, concurrent hypokalemia diminishes I_{Kr} channel activity and further increases inhibition by the macrolide antibiotic. Third, female gender is an independent risk factor, possibly due to gender-specific differences in I_{Kr} density, as seen in rabbit ventricular myocytes (Makkar et al., 1993; Drici et al., 1998). Our results support the idea that acquired arrhythmia can result from inheritance of a mutant channel subunit that reduces cardiac repolarization capacity but is well tolerated until provocative stimuli further decrease the ability of the myocardium to repolarize normally.

Experimental Procedures

Molecular Biology Methods

NCBI databases searched using BLAST algorithms failed to find genes significantly homologous to *KCNE1* (MinK). Reevaluation of sequences below the threshold for significance identified nine ESTs carrying a short target motif. Target amino acids were those in rat MinK known to influence I_{Ks} channel gating (T59, I62, R68, S69, K71, S75, and D77) (Takumi et al., 1991; Splawski et al., 1997), ion selectivity (F55 and T59) (Goldstein and Miller, 1991; Tai and Goldstein, 1998), unitary conductance (S75 and D77) (Sesti and Goldstein, 1998), pore blockade (Y47, I48, F55, G56, and F57) (Goldstein and Miller, 1991; Wang et al., 1996; Tai and Goldstein, 1998), and those that gain exposure in the deep I_{Ks} channel conduction pathway (F55, G56, F57, and T59) (Wang et al., 1996; Tai and Goldstein, 1998). The rat and human sequences encoding MiRP1 were first isolated by reverse transcription from cardiac poly(A)$^+$ mRNA (Clontech). Rapid amplification of cDNA ends was performed with a Marathon cDNA Kit, and random and oligo(dT)-primed adult human heart and adult rat cDNA libraries were screened (Clontech) to determine complete sequences. Three cDNAs for rat and human MiRP1 were isolated and sequenced on both strands. Alignments were performed with ClustalW 1.6 using Blossum algorithms and gap opening and extension penalties of 15 and 0.1. As the gene for MinK is designated *KCNE1*, the novel genes have been assigned *KCNE2* (MiRP1), *KCNE3* (MiRP2), and *KCNE4* (MiRP3) by the Genome Database Nomenclature Committee (HUGO/GDB). The accession numbers for human MiRP1, rat MiRP1, human MiRP2, mouse MiRP2, and mouse MiRP3 are AF071002, AF071003, AF076531, AF076532, and AF076533, respectively.

All cRNAs were synthesized after the genes were ligated into pBF2 with a modified MCS (pGA1) (Sesti and Goldstein, 1998). For SSCP analyses, PCR and DNA sequencing were as described, condition 2 (Splawski et al., 1998); genomic samples were amplified using three primer pairs: 1F, 5′-CCGTTTTCCTAACCTTGTTCG-3′ and 2R, 5′-AGCATCAACTTTGGCTTGGAG-3′; 3F, 5′-GTCTTCCGAA GGATTTTTATTAC-3′ and 4R, 5′-GTTCCCGTCTCTTGGATTTCA-3′; 5F, 5′-AATGTTCTCTTTCATCATCGTG-3′ and 6R, 5′-TGTCTGGAC GTCAGATGTTAG-3′.

Electrophysiology Methods

Xenopus laevis oocytes were injected with cRNA (Sesti and Goldstein, 1998) and whole-cell currents measured 2–4 days after injection of 1 ng *HERG* cRNA with or without 0.2 ng rat or human *MiRP1* cRNA using a two-electrode voltage clamp (Warner Instruments, CT), an IBM computer, and noncommercial software. Data were sampled at 4 kHz and filtered at 1 kHz unless otherwise noted. Raw data are shown without leak correction. Single-channel records were recorded using an Axopatch 200 A amplifier (Axon Instruments, CA), a Quadra 800 computer, and ACQUIRE software (Instrutech, NY) and stored unfiltered on VHS tape. The data were filtered through a four-pole Bessel filter prior to analysis using TAC (Instrutech) or IGOR (WaveMetrics, OR). All experiments were performed at 22°C.

Protocols

Holding voltage in all cases was −80 mV. (1) Steady-state activation; prepulse for 3 s from −80 to 40 mV in 10 mV steps, test pulse for 6 s to −100 mV; interpulse interval, 5 s. (2) Activation kinetics; incremental prepulse durations from 0.005 to 3 s at 0 to 60 mV in 20 mV steps, test pulse for 3 s at −100 mV; interpulse interval, 5 s. (3) Peak current; steady-state deactivation; deactivation kinetics; prepulse for 3 s to 30 mV, test pulse for 5 s from −150 to 10 mV in 10 mV steps; pulse to −120 mV for 1 s; interpulse interval, 5 s. (4) Steady-state inactivation; prepulse for 3 s to 20 mV, pulse for 30 ms from to −120 to 60 mV in 10 mV steps; test pulse for 1 s at 20 mV; interpulse interval, 2 s. (5) E-4031 blockade; 50 cycles were

repeated: pulse for 3 s to 30 mV, test pulse for 5 s to −100 mV. (6) Isochronal and peak currents; pulse for 1 or 2 s from −80 to 20 or 40 mV in steps of 10 mV followed by a 2 s step to −40 mV with a 3 s interpulse interval. (7) Single channels were activated by a 2 s pulse from −80 to 20 mV followed by a test pulse of 4 or 6 s to voltages from −120 to −20 mV in steps of 10 mV with a 3 s interpulse interval.

Ionic Conditions

Activation of channels formed only with HERG or containing both rMiRP1 and HERG subunits was assessed at various Ca^{2+} concentrations. Treating Ca^{2+} as a blocking ion, the apparent K_i for HERG channels was 0.29 ± 0.02 mM at −100 mV, a value similar to that reported by others (Ho et al., 1998), while heteromeric channels containing rMiRP1 had a ~3-fold lower K_i. Initial characterizations were performed in (in mM) 95 KCl, 5 NaCl, 1 $MgCl_2$, 0.3 $CaCl_2$, and 10 HEPES (pH 7.6) with NaOH. Solutions based on levels of ionized species found in human plasma contained (in mM) 4 KCl, 95 NaCl, 0.75 $MgCl_2$, 1 $CaCl_2$, and 10 HEPES (pH 7.6) with NaOH. For K^+ titrations in Figure 4, NaCl and KCl were isotonically substituted. For cell-attached patches, pipette solution was (in mM) 100 KCl, 1 $MgCl_2$, 0.3 $CaCl_2$, 10 HEPES (pH 7.5) with KOH. For whole cell, pipettes contained (in mM) 100 KCl, 1 $MgCl_2$, 10 HEPES, 2 EGTA (pH 7.5) with KOH. A 50 mM Clarithromycin (American Bioanalytical, MA) stock in DMSO was diluted in bath solution while Quinidine and E-4031 were directly dissolved. Hill coefficients were determined according to $1/(1 + ([drug]/K_i)^n)$.

Biochemistry Methods

rMiRP1 and HERG were epitope tagged by replacing the terminal stop codon in each with nucleotides encoding HA residues (YPYDVPDYAX) or cmyc residues (ISMEQKLISEEDLNX). Transient transfection of COS cells was by DEAE-Detran, chloroquine, and DMSO shock. Transfected cells were lysed in buffer A (in mM): 150 NaCl, 1% NP-40, 1% CHAPS, 0.2 PMSF, 20 NaF, 10 Na_3VO_4, 50 Tris (pH 7.4), and 0.7 μg/ml Pepstatin, before being clarified by centrifugation at 10,000 g for 30 s. Immunoprecipitations were carried out with anti-cmyc monoclonal antibody 9E10 (Oncogene Research) and immobilized protein A/G (Pierce). Samples were separated by SDS–PAGE (10%–16%). Western blots were performed with anti-HA monoclonal antibody 12CA5 (Boehringer) with a horseradish peroxidase-chemoluminescence coupled secondary antibody (Oncogene Research) for fluorography. Speedread Lysate 2 (Novagen) rabbit reticulocyte lysate was used to generate protein subunits from cRNAs for rMiRP1, rMinK, and HERG-cmyc. Subunits were radiolabeled with ^{35}S-methionine (Amersham) and diluted in buffer A containing 1.5% NP-40. Binding assays were performed by mixing equal volumes of the reaction mixtures and incubating for 2 hr on ice prior to IP as above.

Acknowledgments

This work was supported by National Institutes of Health grants to S. A. N. G.; G. W. A. is supported by a Wellcome Trust Prize Traveling Fellowship. Support was provided to M. T. K. by the NHLBI, RO1-HL46401, P50-HL52338, MO1-RR00064, and by an award from Bristol-Myers Squibb. We are grateful to M. Sanguinetti for suggesting a key experiment and his insightful feedback during preparation of the manuscript. We thank T. Jentsch for the KCNQ2 clone and R. Goldstein, A. Black, D. Roden, and H. Strauss for thoughtful discussions. We also wish to thank the SADS foundation and Dr. G. Michael Vincent and Dr. Scott Hessen for referring patients.

Received December 24, 1998; revised March 26, 1999.

References

Antzelevitch, C., Sun, Z.Q., Zhang, Z.Q., and Yan, G.X. (1996). Cellular and ionic mechanisms underlying erythromycin-induced long QT intervals and torsade de pointes. J. Am. Coll. Cardiol. *28*, 1836–1848.

Blumenthal, E.M., and Kaczmarek, L.K. (1994). The minK potassium channel exists in functional and nonfunctional forms when expressed in the plasma membrane of *Xenopus* oocytes. J. Neurosci. *14*, 3097–3105.

Busch, A.E., Varnum, M.D., North, R.A., and Adelman, J.P. (1992). An amino acid mutation in a potassium channel that prevents inhibition by protein kinase C. Science *255*, 1705–1707.

Busch, A.E., Busch, G.L., Ford, E., Suessbrich, H., Lang, H.J., Greger, R., Kunzelmann, K., Attali, B., and Stuhmer, W. (1997). The role of the IsK protein in the specific pharmacological properties of the I_{Ks} channel complex. Br. J. Pharmacol. *122*, 187–189.

Carmeliet, E. (1992). Voltage- and time-dependent block of the delayed K^+ current in cardiac myocytes by dofetilide. J. Pharmacol. Exp. Ther. *262*, 809–817.

Carmeliet, E. (1993). Use-dependent block and use-dependent unblock of the delayed rectifier K^+ current by almokalant in rabbit ventricular myocytes. Circ. Res. *73*, 857–868.

Chen, J., Zou, A., Splawski, I., Keating, M.T., and Sanguinetti, M.C. (1999). Long QT syndrome-associated mutations in the Per-Arnt-Sim (PAS) domain of HERG potassium channels accelerate deactivation. J. Biol. Chem. *274*, 10113–10118.

Curran, M.E., Splawski, I., Timothy, K.W., Vincent, G.M., Green, E.D., and Keating, M.T. (1995). A molecular basis for cardiac arrhythmia: HERG mutations cause long QT syndrome. Cell *80*, 795–803.

Daleau, P., Lessard, E., Groleau, M.F., and Turgeon, J. (1995). Erythromycin blocks the rapid component of the delayed rectifier potassium current and lengthens repolarization of guinea pig ventricular myocytes. Circulation *91*, 3010–3016.

Drici, M.D., Knollmann, B.C., Wang, W.X., and Woosley, R.L. (1998). Cardiac actions of erythromycin: influence of female sex. JAMA *280*, 1774–1776.

Duggal, P., Vesely, M.R., Wattanasirichaigoon, D., Villafane, J., Kaushik, V., and Beggs, A.H. (1998). Mutation of the gene for IsK associated with both Jervell and Lange-Nielsen and Romano-Ward forms of Long-QT syndrome. Circulation *97*, 142–146.

Goldstein, S.A., and Miller, C. (1991). Site-specific mutations in a minimal voltage-dependent K^+ channel alter ion selectivity and open-channel block. Neuron *7*, 403–408.

Ho, W.K., Earm, Y.E., Lee, S.H., Brown, H.F., and Noble, D. (1996). Voltage- and time-dependent block of delayed rectifier K^+ current in rabbit sino-atrial node cells by external Ca^{2+} and Mg^{2+}. J. Physiol. *494*, 727–742.

Ho, W.K., Kim, I., Lee, C.O., and Earm, Y.E. (1998). Voltage-dependent blockade of HERG channels expressed in *Xenopus* oocytes by external Ca^{2+} and Mg^{2+}. J. Physiol. *507*, 631–638.

Howarth, F.C., Levi, A.J., and Hancox, J.C. (1996). Characteristics of the delayed rectifier K current compared in myocytes isolated from the atrioventricular node and ventricle of the rabbit heart. Pflugers Arch. *431*, 713–722.

Kaczmarek, L.K., and Blumenthal, E.M. (1997). Properties and regulation of the minK potassium channel protein. Physiol. Rev. *77*, 627–641.

Lee, K.L., Jim, M.H., Tang, S.C., and Tai, Y.T. (1998). QT prolongation and torsades de pointes associated with clarithromycin. Am. J. Med. *104*, 395–396.

Lees-Miller, J.P., Kondo, C., Wang, L., and Duff, H.J. (1997). Electrophysiological characterization of an alternatively processed ERG K^+ channel in mouse and human hearts. Circ. Res. *81*, 719–726.

Liu, S., Rasmusson, R.L., Campbell, D.L., Wang, S., and Strauss, H.C. (1996). Activation and inactivation kinetics of an E-4031-sensitive current from single ferret atrial myocytes. Biophys. J. *70*, 2704–2715.

London, B., Trudeau, M.C., Newton, K.P., Beyer, A.K., Copeland, N.G., Gilbert, D.J., Jenkins, N.A., Satler, C.A., and Robertson, G.A. (1997). Two isoforms of the mouse ether-a-go-go-related gene coassemble to form channels with properties similar to the rapidly activating component of the cardiac delayed rectifier K^+ current. Circ. Res. *81*, 870–878.

Makkar, R.R., Fromm, B.S., Steinman, R.T., Meissner, M.D., and Lehmann, M.H. (1993). Female gender as a risk factor for torsades de pointes associated with cardiovascular drugs. JAMA *270*, 2590–2597.

McDonald, T.V., Yu, Z., Ming, Z., Palma, E., Meyers, M.B., Wang, K.W., Goldstein, S.A.N., and Fishman, G.I. (1997). A minK-HERG

complex regulates the cardiac potassium current I_{Kr}. Nature *388*, 289–292.

Roden, D.M. (1998). Taking the idio out of idiosyncratic—predicting torsades de pointes. Pacing Clin. Electrophysiol. *21*, 1029–1034.

Roden, D.M., Woosley, R.L., and Primm, R.K. (1986). Incidence and clinical features of the quinidine-associated long QT syndrome: implications for patient care. Am. Heart J. *111*, 1088–1093.

Sanguinetti, M.C., and Jurkiewicz, N.K. (1992). Role of external Ca^{2+} and K^+ in gating of cardiac delayed rectifier K^+ currents. Pflugers Arch. *420*, 180–186.

Sanguinetti, M.C., Jiang, C., Curran, M.E., and Keating, M.T. (1995). A mechanistic link between an inherited and an acquired cardiac arrhythmia: HERG encodes the I_{Kr} potassium channel. Cell *81*, 299–307.

Sanguinetti, M.C., Curran, M.E., Spector, P.S., and Keating, M.T. (1996a). Spectrum of HERG K^+-channel dysfunction in an inherited cardiac arrhythmia. Proc. Natl. Acad. Sci. USA *93*, 2208–2212.

Sanguinetti, M.C., Curran, M.E., Zou, A., Shen, J., Spector, P.S., Atkinson, D.L., and Keating, M.T. (1996b). Coassembly of K(V)Lqt1 and Mink (Isk) proteins to form cardiac I-Ks potassium channel. Nature *384*, 80–83.

Scamps, F., and Carmeliet, E. (1989). Delayed K^+ current and external K^+ in single cardiac Purkinje cells. Am. J. Physiol. *257*, C1086–C1092.

Schulze-Bahr, E., Wang, Q., Wedekind, H., Haverkamp, W., Chen, Q., and Sun, Y. (1997). KCNE1 mutations cause Jervell and Lange-Nielsen syndrome. Nat. Genet. *17*, 267–268.

Sesti, F., and Goldstein, S.A.N. (1998). Single-channel characteristics of wildtype I_{Ks} channels and channels formed with two minK mutants that cause long QT syndrome. J. Gen. Phys. *112*, 651–664.

Shibasaki, T. (1987). Conductance and kinetics of delayed rectifier potassium channels in nodal cells of the rabbit heart. J. Physiol. *387*, 227–250.

Smith, P.L., Baukrowitz, T., and Yellen, G. (1996). The inward rectification mechanism of the HERG cardiac potassium channel. Nature *379*, 833–836.

Snyders, D.J., and Chaudhary, A. (1996). High affinity open channel block by dofetilide of HERG expressed in a human cell line. Mol. Pharmacol. *49*, 949–955.

Spector, P.S., Curran, M.E., Keating, M.T., and Sanguinetti, M.C. (1996a). Class III antiarrhythmic drugs block HERG, a human cardiac delayed rectifier K^+ channel. Open-channel block by methanesulfonanilides. Circ. Res. *78*, 499–503.

Spector, P.S., Curran, M.E., Zou, A., Keating, M.T., and Sanguinetti, M.C. (1996b). Fast inactivation causes rectification of the I_{Kr} channel. J. Gen. Physiol. *107*, 611–619.

Splawski, I., Tristani-Firouzi, M., Lehmann, M.H., Sanguinetti, M.C., and Keating, M.T. (1997). Mutations in the hminK gene cause long QT syndrome and suppress I_{Ks} function. Nat. Genet. *17*, 338–340.

Splawski, I., Shen, J., Timothy, K.W., Vincent, G.M., Lehmann, M.H., and Keating, M.T. (1998). Genomic structure of three long QT syndrome genes: KVLQT1, HERG, and KCNE1. Genomics *51*, 86–97.

Tai, K.K., and Goldstein, S.A.N. (1998). The conduction pore of a cardiac potassium channel. Nature *391*, 605–608.

Tai, K.-K., Wang, K.-W., and Goldstein, S.A.N. (1997). MinK potassium channels are heteromultimeric complexes. J. Biol. Chem. *272*, 1654–1658.

Takumi, T., Ohkubo, H., and Nakanishi, S. (1988). Cloning of a membrane protein that induces a slow voltage-gated potassium current. Science *242*, 1042–1045.

Takumi, T., Moriyoshi, K., Aramori, I., Ishii, T., Oiki, S., Okada, Y., Ohkubo, H., and Nakanishi, S. (1991). Alteration of channel activities and gating by mutations of slow ISK potassium channel. J. Biol. Chem. *266*, 22192–22198.

Trudeau, M.C., Warmke, J.W., Ganetzky, B., and Robertson, G.A. (1995). HERG, a human inward rectifier in the voltage-gated potassium channel family. Science *269*, 92–95.

Tyson, J., Tranebjaerg, L., Bellman, S., Wren, C., Taylor, J.F., Bathen, J., Aslaksen, B., Sorland, S.J., Lund, O., Malcolm, S., et al. (1997). IsK and KvLQT1: mutation in either of the two subunits of the slow component of the delayed rectifier potassium channel can cause Jervell and Lange-Nielsen syndrome. Hum. Mol. Genet. *6*, 2179–2185.

Veldkamp, M.W., van Ginneken, A.C., Opthof, T., and Bouman, L.N. (1995). Delayed rectifier channels in human ventricular myocytes. Circulation *92*, 3497–3504.

Vetter, D.E., Mann, J.R., Wangemann, P., Liu, J., McLaughlin, K.J., Lesage, F., Marcus, D.C., Lazdunski, M., Heinemann, S.F., and Barhanin, J. (1996). Inner ear defects induced by null mutation of the isk gene. Neuron *17*, 1251–1264.

Wang, K.W., and Goldstein, S.A.N. (1995). Subunit composition of minK potassium channels. Neuron *14*, 1303–1309.

Wang, K.-W., Tai, K.-K., and Goldstein, S.A.N. (1996). MinK residues line a potassium channel pore. Neuron *16*, 571–577.

Wang, S., Liu, S., Morales, M.J., Strauss, H.C., and Rasmusson, R.L. (1997a). A quantitative analysis of the activation and inactivation kinetics of HERG expressed in *Xenopus* oocytes. J. Physiol. *502*, 45–60.

Wang, S., Morales, M.J., Liu, S., Strauss, H.C., and Rasmusson, R.L. (1997b). Modulation of HERG affinity for E-4031 by $[K^+]o$ and C-type inactivation. FEBS Lett. *417*, 43–47.

Wollnik, B., Schroeder, B.C., Kubisch, C., Esperer, H.D., Wieacker, P., and Jentsch, T.J. (1997). Pathophysiological mechanisms of dominant and recessive KVLQT1 K^+ channel mutations found in inherited cardiac arrhythmias. Hum. Mol. Genet. *6*, 1943–1949.

Yang, T., and Roden, D.M. (1996). Extracellular potassium modulation of drug block of I_{Kr}. Implications for torsade de pointes and reverse use-dependence. Circulation *93*, 407–411.

Yang, Y., and Sigworth, F. (1998). Single-channel properties of I_{Ks} potassium channels. J. Gen. Physiol. *112*, 665–678.

Yang, T., Wathen, M.S., Felipe, A., Tamkun, M.M., Snyders, D.J., and Roden, D.M. (1994). K^+ currents and K^+ channel mRNA in cultured atrial cardiac myocytes (AT-1 cells). Circ. Res. *75*, 870–878.

Yang, T., Snyders, D.J., and Roden, D.M. (1997). Rapid inactivation determines the rectification and $[K^+]o$ dependence of the rapid component of the delayed rectifier K^+ current in cardiac cells. Circ. Res. *80*, 782–789.

Zhou, Z., Gong, Q., Ye, B., Fan, Z., Makielski, J.C., Robertson, G.A., and January, C.T. (1998). Properties of HERG channels stably expressed in HEK 293 cells studied at physiological temperature. Biophys. J. *74*, 230–241.

Zou, A., Curran, M.E., Keating, M.T., and Sanguinetti, M.C. (1997). Single HERG delayed rectifier K^+ channels expressed in *Xenopus* oocytes. Am. J. Physiol. *272*, H1309–H1314.

GenBank Accession Numbers

The accession numbers for human MiRP1 (*hKCNE2*), rat MiRP1 (*rKCNE2*), human MiRP2 (*hKCNE3*), mouse MiRP2 (*mKCNE3*), and mouse MiRP3 (*mKCNE4*) are AF071002, AF071003, AF076531, AF076532, and AF076533, respectively.